

ARTICLE OPEN



Physics-based modeling of climate change impact on hurricane-induced coastal erosion hazards

Mohammad Jamous¹, Reza Marsooli^{1✉} and Jon K. Miller¹

Coastal erosion is an adverse impact of extreme water levels during major hurricanes. A warmer climate is expected to increase storm surge and wave hazards due to hurricane climatology change (HCC) and sea level rise (SLR). We conduct physics-based morphodynamic modeling to quantify the regional impacts of HCC and SLR on erosion hazards to sandy beaches and dunes along the barrier islands of New Jersey in the United States. Under the RCP8.5 scenario, we find a substantial increase in erosion hazards from the late-20th-century to late-21st-century. The regionally averaged 100-year eroded volume of beach-dune systems would increase by 58 and 84%, respectively, under the HCC and HCC + SLR scenarios. Our projections show a large spatial variability in future changes to erosion hazards, suggesting that, in addition to HCC and SLR, the morphological characteristics of beach-dune systems play an important role in the impacts of climate change on coastal erosion.

npj Climate and Atmospheric Science (2023)6:86; <https://doi.org/10.1038/s41612-023-00416-0>

INTRODUCTION

Tropical cyclones and especially intense hurricanes pose a significant threat to coastal regions, mainly due to the destructive hydrodynamic forces of storm surges and wind-generated waves. Within a short period of time, such forcings can cause severe coastal erosion, overtopping of dunes and coastal structures, and flooding^{1–3}. For example, Hurricane Irma in 2017 caused 1–1.5 m vertical losses of the beach-dune systems in the Virgin Islands, as well as a 6–8 m coastline retreat⁴.

Global warming is expected to impact the intensity and frequency of hurricanes and, consequently, the hydrodynamic forces exerted on coastal areas. Previous studies have found that the intensity of tropical cyclones (TCs) would increase under a future warming climate^{5–7}. While the overall frequency of TCs is expected to decrease in a warmer climate, the frequency of major and very intense hurricanes (Saffir-Simpson categories 3–5) is expected to increase^{8,9}. Sugi et al.¹⁰ concluded that under a warmer climate, the number of days with major TCs would increase in most regions in the Northern Hemisphere except for the southwestern part of the Northwest Pacific, the Northeast Pacific, and the westernmost part of the North Atlantic. Stronger and more frequent major hurricanes would result in larger threats from storm surges and energetic wind waves, which, in turn, could cause more severe coastal impacts.

In addition to the Hurricane Climatology Change (HCC), global warming would result in Sea Level Rise (SLR). The sixth report of the Intergovernmental Panel on Climate Change projects an increase of 0.63–1.01 m in the late-21st-century global mean sea level relative to the 1995–2014 baseline¹¹. Depending on the geographical location, local SLR can differ from global SLR due to local factors such as ocean currents and land elevation change due to subsidence or uplifting. For example, between 1911 and 2019, the mean sea level rose 0.45 m at Atlantic City, New Jersey (located northeast of the U.S.) while the total increase in the global mean sea level¹² shows a 0.19 m. SLR projections also show that the future local SLR in many regions worldwide will substantially depart from the global sea level rise projections¹³. A higher mean

sea level will alter the bathymetry, which can influence wave characteristics in the present-day nearshore zones.

Climate change impact studies have shown that the combined effect of HCC and SLR would significantly change future storm surge and wave hazards in coastal regions^{14–18}. Marsooli et al.¹⁷ quantified the effect of HCC and SLR on wind waves generated by major hurricanes off the coast of New Jersey, U.S. They found that there would be a statistically significant increase in wave heights from a historical period in the late 20th century (1980–2000) to a future period in the late 21st century (2080–2100) under a high greenhouse gas emission scenario. They concluded that while HCC would dominate the wave height increase in deep waters, the effect of SLR on wave heights in the present-day nearshore zone would dominate the effect of HCC.

The combined effect of HCC and SLR (hereafter HCC + SLR) on wave characteristics in the nearshore zone could affect hurricane-induced erosion hazards to beach-dune systems in coastal areas. However, a quantitative understanding of such effects is limited. This is due to the challenges in quantifying the response of storm-induced erosion hazards to HCC and SLR. One challenge is the high computational cost of modeling morphodynamic processes during storm events. To overcome this challenge, some studies have used simplified methods such as the Bruun rule to quantify the response of coastal erosion hazards to climate change^{3,14,19}. However, the validity of findings based on these simplified methods has been questioned by the scientific community²⁰. Physics-based numerical models provide an accurate alternative approach, but these models are difficult to calibrate and computationally expensive, especially for regional or global-scale climate impact studies. The computational cost, however, could be reduced by applying these models to a series of one-dimensional cross-shore profiles that resolve the spatial variation in the characteristics of beach-dune systems in the study area. A one-dimensional simulation is a reliable approach, given that morphological changes during storms are mainly the result of cross-shore sediment transport²¹.

The other challenge in projecting the impact of climate change on hurricane-induced coastal erosion is the availability of storm

¹Department of Civil, Environmental, and Ocean Engineering, Stevens Institute of Technology, Hoboken, NJ 07030, USA. ✉email: rmarsool@stevens.edu

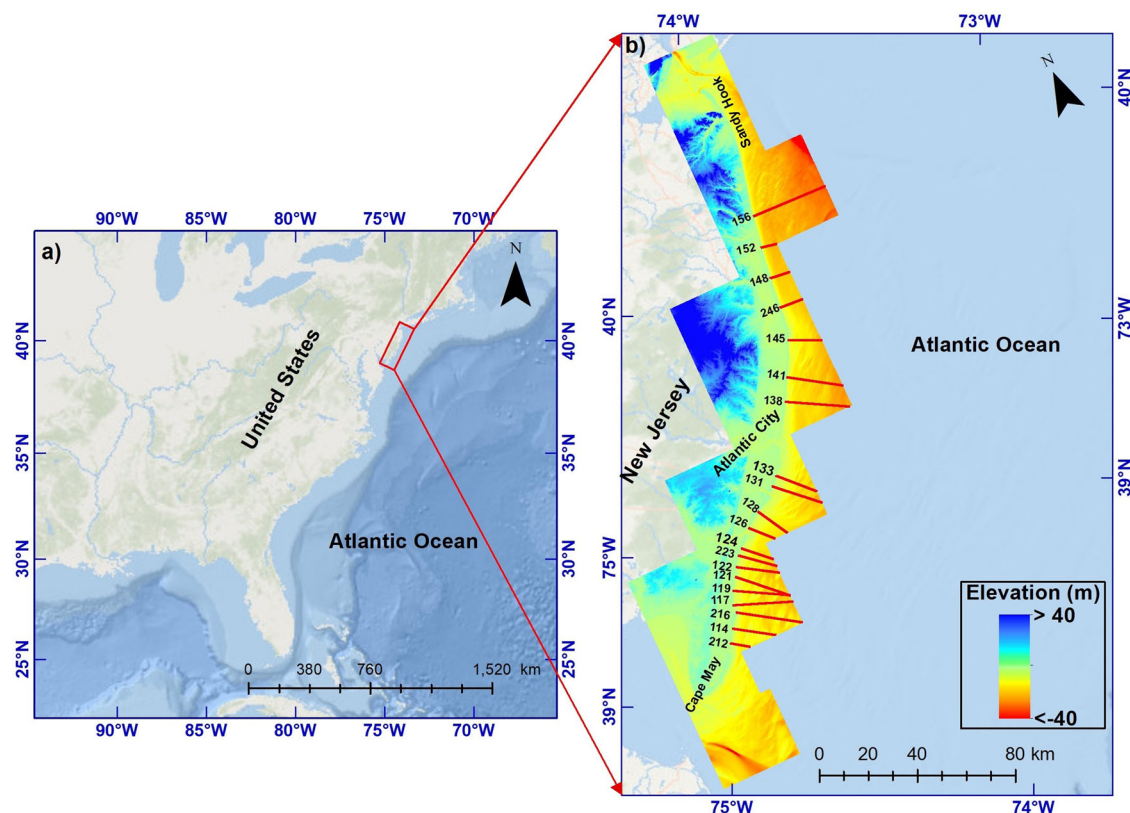


Fig. 1 Study area. **a** Shows the location of the study area (red rectangle) with respect to the United States and the Atlantic Ocean. **b** A close-up view of the study area, the selected cross-shore profiles (red line in the right panel), profile ID numbers, and the digital elevation model.

datasets that accurately account for future changes in hurricane climatology. Some studies have directly utilized atmospheric forcings from Global Climate Models (GCMs) to project the effects of global warming on coastal erosion²². While these studies advance the understanding of climate change impacts, their findings are most valid for coastal erosion hazards due to non-tropical cyclones, given that the spatial resolution of most GCMs is coarse for resolving TCs. Fine-resolution decadal-to-century-long climate simulation is computationally expensive and is likely to remain a challenge, as exemplified by a much larger number of climate models with a coarse resolution than fine resolution used in climate studies²³. An alternative approach to generating hurricane datasets is the use of statistical/deterministic hurricane models such as the model developed by Emanuel et al.⁵. These models generate synthetic storms for given large-scale oceanic and atmospheric conditions, which can be obtained from GCMs projections. Such synthetic storms have been successfully used in the assessment of the climate change impact on hurricane storm surge and wave hazards^{16,17,24}.

This study adopts a physics-based modeling approach (see section “Methods: Numerical model”) to project climate change impacts on hurricane-induced coastal erosion hazards to sandy beaches and dunes. With a focus on a regional-scale study area in New Jersey, U.S. (Fig. 1), we quantify the effects of HCC and SLR on hurricane-induced erosion hazards to sandy beach-dune systems. We use a comprehensively calibrated XBeach-surfbeat model²⁵ to simulate hurricane-induced coastal erosion along 20 cross-shore profiles (Fig. 1). Simulations are carried out for an ensemble of synthetic major hurricanes (categories 3–5) for the historical period of 1980–2000 and the future period of 2080–2100 under the Representative Concentration Pathway 8.5 (RCP8.5) scenario. The synthetic hurricanes are based on the datasets from Marsooli and Lin²⁶, which were generated by the statistical/deterministic

hurricane model⁵ for the Atlantic basin. The hurricane datasets were generated for the climate projections based on four CMIP5 GCMs (see section “Methods: Synthetic hurricanes and SLR scenario”). Physics-based modeling of the combined effects of HCC and SLR is performed for an SLR scenario of 1.19 m, which has a 50% chance of being equalled or exceeded (under the RCP8.5 scenario) in the study area by the end of the century¹².

Erosion hazards to beach-dune systems are quantified using the Total Eroded Volume (TEV) metric (in percentage), which is defined based on the ratio of the total volume of eroded sand to the initial total volume of sand in the beach-dune system (see section “Methods: Erosion hazard metrics”). We also use a damage classification metric²⁷ to quantify changes in the probability of beach-dune damage at different levels.

RESULTS

Figure 2 shows a statistical summary of the TEV metric calculated based on the simulated post-storm profiles (e.g., gray lines in Supplementary Fig. 1) for the historical and future periods. In general, our results show an increase in erosion hazards from the historical to future periods under both HCC and HCC + SLR scenarios. While the mean and maximum TEVs averaged across all profiles are, respectively, 5% and 27% in the historical period, they increase to 5.4% and 32% in the future period under HCC and 9% and 48% under the combined HCC and SLR scenario. Under the HCC scenario, the future increase in TEV is due to the increase in the intensity and frequency of the hurricanes in the study area¹⁷, increasing hydrodynamic forcings due to storm surges and waves exerted on beach-dune systems. Under the HCC + SLR scenario, future increases in erosion hazards are also attributed to a deeper present-day near-shore zone, which will allow more energetic waves to reach shorelines.

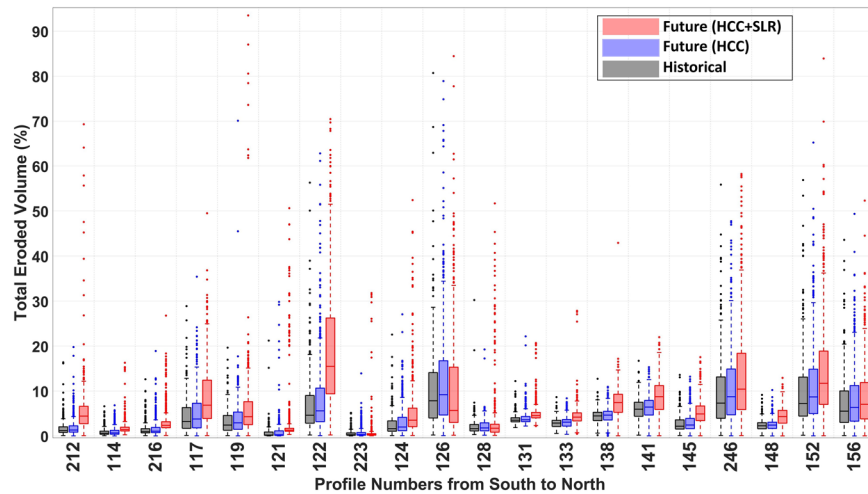


Fig. 2 Total Eroded Volume (TEV) calculated for the hurricane datasets of historical and future periods. Boxes represent the first quartile to the third quartile. The horizontal line in each box represents the median value. The whiskers represent the minimum and maximum values, which are not outliers. Dot markers represent outliers.

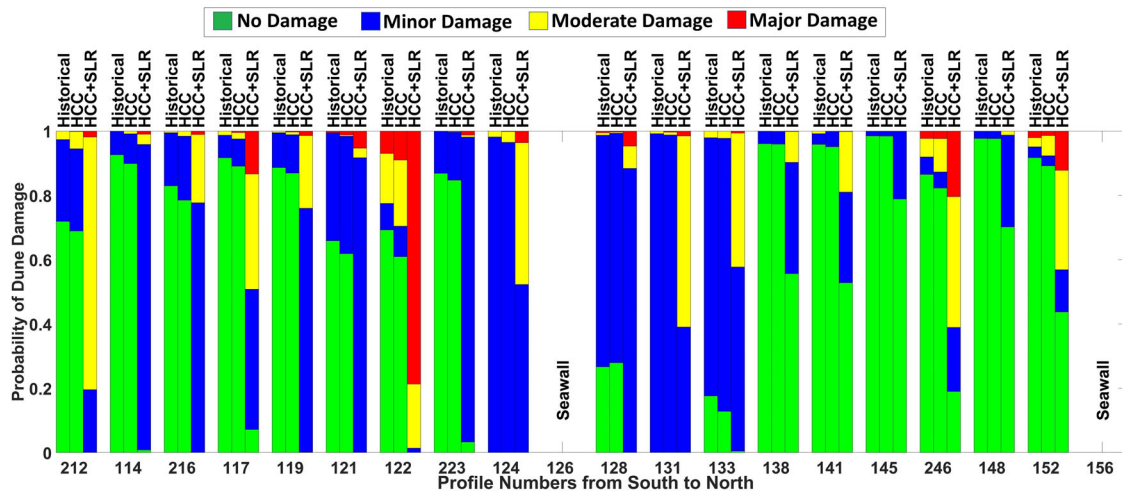


Fig. 3 Probability of dune damage classes. Each group of three columns represents one profile. The first stacked column for each profile represents the probabilities of damage classes in the historical period. The second and third columns represent probabilities of damage classes in the future period under HCC and HCC + SLR, respectively.

In most profiles, the effect of SLR on the projected increases in future erosion hazards dominates the effect of HCC. Our results also suggest that the characteristics of beach-dune systems also play an important role in changes to erosion hazards. For example, the largest effect of SLR is projected for Profile 122 (Supplementary Fig. 1g), which is characterized by a narrow beach (Supplementary Fig. 2d), compared to other profiles. Such a narrow beach would allow larger waves to reach the dune under the SLR scenario, resulting in a significant dune erosion hazard at this location. In contrast to other sites, at Profile 126 (Supplementary Fig. 1j), the projected increase in TEV under HCC + SLR is smaller than that calculated under HCC. This is because of the absence of a dune at this location. Instead, this profile is characterized by a beach-seawall system (Supplementary Fig. 2a). A large portion of the narrow beach (79 m wide) at this location becomes inundated under the SLR scenario, resulting in less severe beach erosion during the simulated hurricanes. Profile 156 (Supplementary Fig. 1t) is also characterized by a beach-seawall system, but the projected TEV under HCC + SLR is larger than that under HCC. This is because the beach at this site is wide (181 m) in which a large portion of the beach remains above the mean sea level under the future SLR scenario, resulting in a large volume of

sand on the beach remaining susceptible to erosion during extreme events.

Figures 3 and 4 show, respectively, the probability of a certain damage category for the dunes and beaches at the study sites. Our results (Fig. 3) show that the probability of major dune damage in the historical period was about zero at most study sites, except at Profiles 122, 246, and 152, where the probabilities of major damage to dunes were 0.07, 0.02, and 0.02, respectively. As HCC causes major hurricanes to increase in intensity and frequency, the probability of dune damage increases. However, at most sites, the state of dune damage remains the same from historical to future periods. For example, if the dune at a specific site was only subject to minor damage in the historical period (e.g., Profile 138), it would remain only subject to minor damage in the future period under the HCC scenario. In contrast, when SLR effects are included (i.e., the HCC + SLR scenario), the state of damage is more likely to change. For example, while the dune at Profile 138 is only subject to minor damage in the historical period and the future period under the HCC scenario, it is subject to a 0.09 probability of moderate damage in the future period under the HCC + SLR scenario.

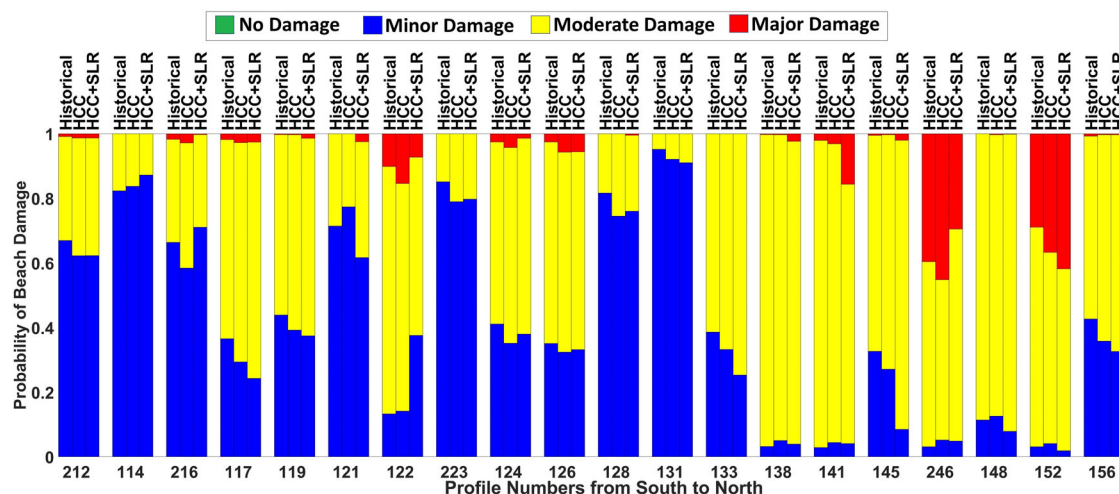


Fig. 4 Probability of beach damage classes. Each group of three columns represents one profile. The first stacked column for each profile represents the probabilities of damage classes in the historical period. The second and third columns represent probabilities of damage classes in the future period under HCC and HCC + SLR, respectively.

In contrast to dunes, we found that it is less likely for beaches to experience changes in the state of damage under the HCC + SLR scenario (Fig. 4). This is because a portion of present-day beaches would be submerged due to SLR and consequently less exposed to direct wave attack and erosion. Results show that most study sites are characterized by a high probability of moderate damage to beaches, while the dunes at these sites are subject to only a small probability of minor damage. For example, under the HCC + SLR scenario, the probabilities of the beach at Profile 138 facing minor, moderate, and major damage are approximately 0.04, 0.93, and 0.03, respectively. Under the same scenario, the damage probabilities for the dune at this location are 0.35, 0.09, and 0. This reiterates the importance of beaches as the first line of coastal defense, suggesting that the vulnerability of beach-dune systems to HCC and HCC + SLR strongly depends on the performance of beaches.

Our results also show that changes in the erosion hazards to beaches are related to changes in the level of damage to dunes. For example, while the probability of major damage to the beach at Profile 122, is 0.1 in the historical period, it increases to 0.15 in the future period under the HCC scenario but decreases to 0.07 in the future period under the HCC + SLR scenario. This is due to the very high increase in the probability of major damage to the dune at this site under the HCC + SLR scenario, causing the eroded sand from the dune to deposit on the beach and reduce the level of damage (characterized in this study by erosion) to the beach. Beach-dune systems at Profiles 216, 124, and 246 show the same behavior.

Figure 5 shows the return period curves of TEV at a series of selected study sites for the historical and future periods (see Supplementary Fig. 5 for other study sites). The results show a substantial increase in erosion hazards to the beach-dune systems. For example, while the best estimate (50th percentile, represented by solid lines in Fig. 5) of the 100-year TEV at Profile 145 is 3% in the historical period, it increases to 5.7 and 8.6% in the future period under HCC and HCC + SLR scenarios, respectively. Across all study sites, the percent increase in the best estimate of 100-year TEV, hereafter ΔTEV_{100-yr} , in the future period is between 25 and 135% (Fig. 6b, c), with a spatially averaged increase of 58 and 84% under the HCC and HCC + SLR scenarios, respectively. The very likely estimates (5th–95th percentiles, i.e., 90% statistical confidence interval) of the 100-year TEV show a relatively large statistical uncertainty. For example, at Profile 145, the very likely estimates of ΔTEV_{100-yr} for the future period under HCC and HCC + SLR scenarios are, respectively, 5–6.2 and 8–9.4%.

The projected ΔTEV_{100-yr} shows substantial spatial variability, with smaller increases in the northern regions and larger increases in the southern regions (Fig. 6). For example, under the HCC scenario, ΔTEV_{100-yr} increases from 4.5% in the northern regions of the study area to 34.7% in the southern regions. Under the HCC + SLR scenario, ΔTEV_{100-yr} increases from 59.2% at sites located in the northern regions to 135% for sites in the south. The north-to-south increasing pattern in hurricane-induced erosion hazards is due to the patterns in the impact of HCC on the extreme wave climate in the study area. Marsooli et al.¹⁷ found that the southern region of the study area would be exposed to larger hurricane-induced waves, due to, a larger number of major hurricanes that impact the lower latitudes of the study area. The bathymetry of shallow waters and the shoreline geometry could be the other controlling factors, which need to be investigated in future studies.

DISCUSSION

Many coastal communities and infrastructure worldwide are protected against storm surges and waves by sandy beach-dune systems, which are susceptible to severe episodic erosion during extreme events. Using a regional-scale modeling study, we found that, under a high-emission scenario, HCC and SLR would cause a substantial increase in hurricane-induced erosion hazards to beaches and dunes. This could, in turn, result in increased exposure of the hinterland to flooding. To mitigate the impacts of climate change on episodic coastal erosion, the beach-dune systems, especially in areas where these systems are the main line of coastal defense, need to be reinforced. A mitigation strategy to be investigated could focus on retaining or widening the beach width through nourishment projects, as our results showed a higher level of damage to dunes that are faced with narrower beaches. Future studies can also examine the effectiveness of other engineering and natural/nature-based approaches, e.g., artificial reefs and hybrid seawall-dune-beach systems, to mitigate the impact of climate change on coastal erosion.

While climate change impacts vary regionally, our results provide findings that are transferable to other regions susceptible to hurricanes. Our results suggest that hurricane climatology change could have a considerable effect on extreme coastal erosion (Fig. 6b). Therefore, while the effects of sea level rise are increasingly being considered in climate risk-informed coastal development, the response of erosion hazards to changes in hurricane intensity and frequency should be also considered in

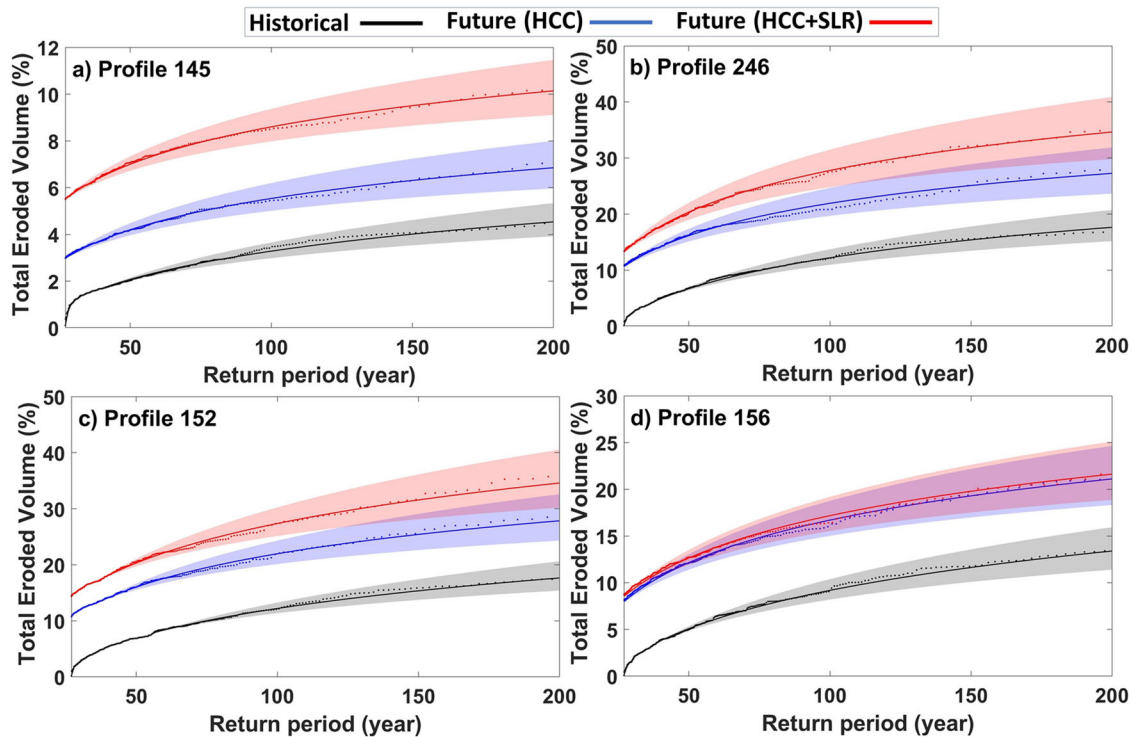


Fig. 5 TEV Return period curves for the selected beach-dune systems. The return periods are shown for profiles **a** 145, **b** 246, **c** 152, and **d** 156. Shaded areas show the 90% confidence interval associated with each fitted curve. Dot markers represent the calculated TEVs from XBeach simulations.

areas with erodible coasts. Our findings also suggest that the extent to which coastal erosion hazards respond to climate change depends on not only changes in erosive forces but also the characteristics of beach-dune systems. For example, our results showed that the erosion hazard metric and the level of damage at the study site Profile 122 which is characterized by a narrow beach in front of the dune were larger than those at the neighboring site Profile 223 which is characterized by a wide beach (Fig. 6c).

We focused on episodic erosion caused by major hurricanes while neglecting other drivers of extreme coastal erosion. This was motivated by findings from previous studies that showed a warmer climate would result in an increase in the intensity of global TCs and a higher frequency of major hurricanes in the Atlantic Ocean. In addition to hurricanes, severe coastal erosion can also occur during extratropical cyclones (ETCs)^{28,29}. For example, the northeastern storm of 2009 is considered one of the most extreme erosion events in the history of New Jersey. Extreme beach erosion occurred due to the long storm duration and exposure time to waves³⁰. While there are different findings among studies concerning global warming impacts on ETCs, several studies have found that the number of ETCs would decrease in a warmer climate. For instance, Zappa et al.³¹ found that a warmer future climate would decrease the frequency of extreme ETCs in the North Atlantic by % in the cold season and by 6% in the warm season. Seiler and Zwiers³² analyzed projections of extratropical storms from CMIP5 climate models and found that the total number of storms in the Atlantic would decrease by about 17% (averaged over all models). Future changes to the intensity of ETCs are further subject to large uncertainties, with a mix of findings on an increase and decrease in the wind intensity of ETCs under an enhanced greenhouse warming^{29,33,34}. Nevertheless, future studies should investigate the response of coastal erosion to ETCs as well as the combined ETC and tropical cyclone climatology change.

In addition to the effects of hurricane climatology change (HCC scenario), we investigated the extent to which the combined effect of HCC and SLR (HCC + SLR scenario) alters the effect of HCC. However, we did not explicitly quantify the contribution of SLR (i.e., SLR-only scenario). The SLR-only contribution may be estimated by subtracting the results of the HCC scenario (e.g., Fig. 6b) from the HCC + SLR scenario (Fig. 6c) but at the cost of neglecting the nonlinear response of coastal processes to a changing mean sea level. Due to the high computational cost of hydrodynamic-wave-morphodynamic modeling, the study considered only one SLR scenario that has a 50% chance to be equalled or exceeded under the high emission scenario¹². Given the availability of probabilistic SLR projections for different emission scenarios, future investigations are needed to account for SLR scenarios with various probabilities of occurrence, which can support coastal resilience planning.

Given the non-stationarity and future deep uncertainties in climate, adaptive coastal management can benefit from a quantitative understanding of changes in coastal hazards under different future time horizons and emission scenarios. Mainly constrained by the high computational cost of physics-based numerical modeling, this study considered only a single time horizon at the end of the 21st century and a high greenhouse gas emission scenario. Future studies are needed to investigate to what extent coastal hazards will respond to hurricane climatology change in different time horizons and under more optimistic emission scenarios. Jing et al.³⁵ found a substantial change in the frequency of Atlantic major hurricanes from an early to late 21st century time horizon. For example, under the RCP4.5 scenario, they found that the frequency of major hurricanes would increase, compared to the baseline of 1986–2005, between 2.2 and 24.0% (projected by different models) in the time horizon of 2016–2023 and between 17.1 and 60.4% in 2081–2100. Furthermore, their results showed a large spread on the projected percentage of increase. While their dynamic modeling approach showed a 60.4%

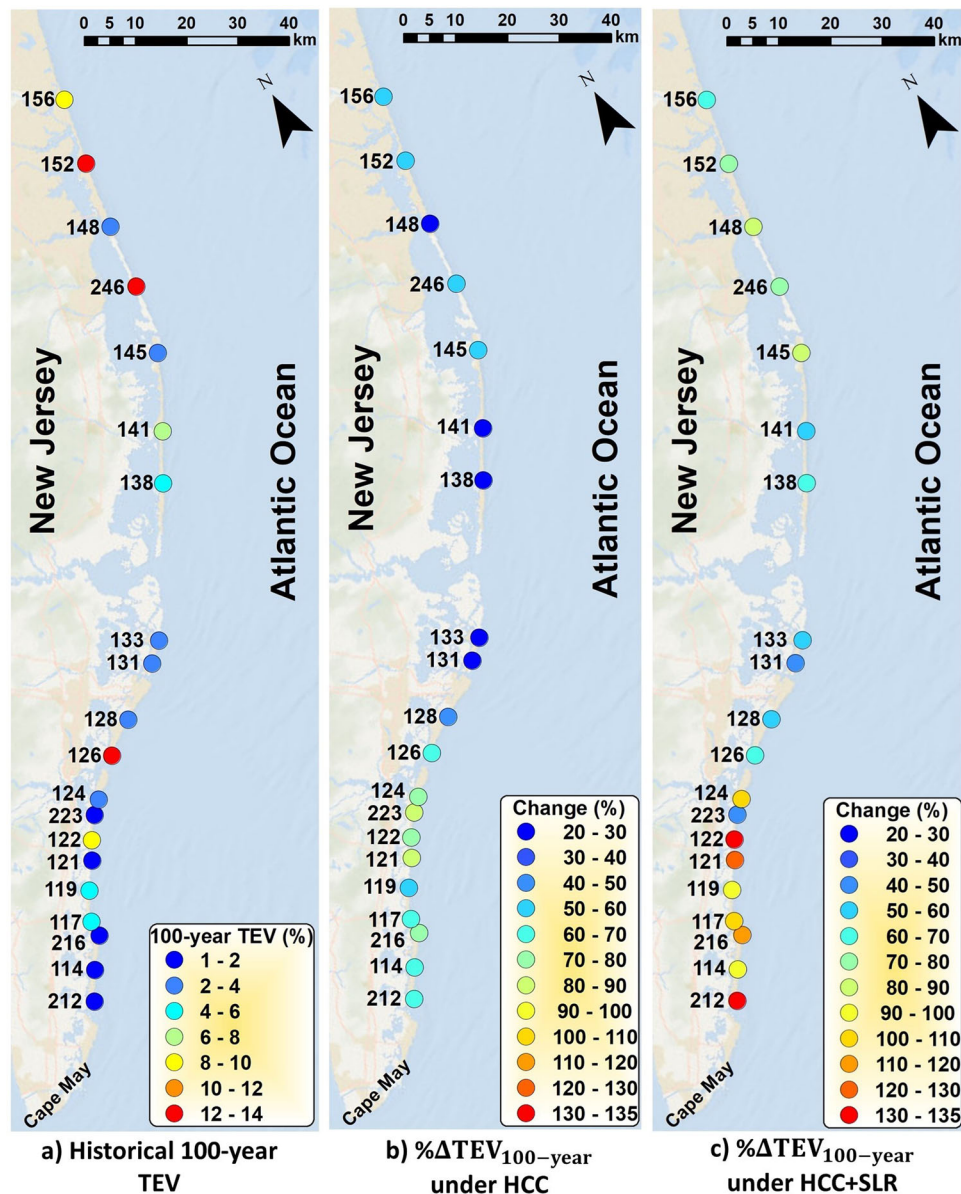


Fig. 6 Spatial variability of changes in the 100-year Total Eroded Volume. **a** The best estimate of 100-year Total Eroded Volume (TEV100-yr) in the historical period, and **b, c** the percent change in TEV100-yr in the future period under HCC and HCC + SLR scenarios.

increase in the frequency of major hurricanes averaged in the Atlantic basin, the statistical and statistical-deterministic synthetic models showed an increase of 17.1 and 37.8%, respectively, by the end of the century. Given that this previous study was carried out at a basin scale, the uncertainties can be larger for landfalling hurricanes. This reiterates the importance of adaptive coastal management since the coastal hazards would be influenced by the uncertainties and non-stationarity of hurricane climatology change.

Process-based numerical models, such as the model adopted in the present study, provide an accurate and robust approach for quantifying the impact of climate change on coastal erosion hazards but at a significant computational cost, which constrained our study from including a wide range of climate change scenarios. Future studies should explore the use of other approaches that provide a cost-effective, yet reliable projection of coastal erosion response to climate change. Data-driven, surrogate models for coastal erosion are a potential candidate for use in erosion hazard studies^{36,37}. These models need to be

carefully developed, given that they are only as accurate as the data used to train them. If the data used to train the surrogate models is limited or does not capture the full range of variability in future storms, the predictions may be unreliable. This is particularly relevant for climate change impact studies, as changes in storms may be experienced in conditions that are outside of the range of data used for the surrogate model development.

METHODS

Numerical model

We use the process-based XBeach model to simulate hurricane-induced morphological changes to beach-dune systems. XBeach is an open-source, coupled hydrodynamic-morphodynamic model that simulates coastal morphological changes on the temporal scale of storms. Depending on the mode, it simulates morphological changes on different wave scales. XBeach can run in hydrostatic, surfbeat, and non-hydrostatic modes. The surfbeat version³⁸ simulates short waves, on the wave group scale, by

solving the short-wave action balance equation. XBeach has been widely adopted to simulate storm-induced erosion in different coastal regions around the globe^{39–41}.

This study uses the one-dimensional XBeach model in its surfbeat mode to simulate coastal erosion from a large number of synthetic major hurricanes described later. The model is forced at its offshore boundary, which is located at a water depth of ~15 m, using hourly time series of storm surge height and frequency-direction wave spectrum. These hourly boundary conditions are obtained from a regional-scale Advanced CIRCulation model (ADCIRC)^{42,43} that is coupled with the Simulating Waves Nearshore model (SWAN)^{44,45}. Marsooli et al.¹⁷ used the coupled ADCIRC + SWAN model to simulate storm surges and waves for the synthetic storms that are used in the present study.

Study area

The study area covers the New Jersey Barrier Islands (NJBIs) in the northeastern U.S. (Fig. 1). These barrier islands are highly developed and populated and are considered the economic engine of New Jersey's tourism industry. Assets and infrastructure on these islands are protected against extreme sea levels by assorted structures and beach-dune systems, which are exposed to episodic coastal erosion caused by storm surges and waves from the Atlantic Ocean. For example, on the 29th of October 2012, Hurricane Sandy generated a maximum storm surge of 2.7 m at the Coast Guard Station in Sandy Hook, New Jersey⁴⁶, and a maximum significant wave height of 9.85 m at NOAA buoy 44025 off the coast of New Jersey. The dunes of NJBIs experienced a vertical loss of 2–6 m and a volume loss between 25 and 150 m³ m⁻¹^{47,48}.

We use the XBeach model to simulate storm-induced morphological changes to beach-dune systems at 20 selected sites in the study area (Fig. 6). Jamous et al.²⁵ have developed and calibrated XBeach models of one-dimensional cross-shore profiles for these sites using beach and dune elevation measurements, collected by the New Jersey Beach Profile Network (NJBPN) program of the New Jersey Department of Environmental Protection, prior to and post Hurricane Sandy. The beach-dune systems at the different sites are a combination of natural, recently nourished, and previously nourished. Each site is characterized by a unique grain size distribution. The median sediment particle size (D50) varies from 0.2 mm to 0.6 mm across different profiles⁴⁹. We provide the XBeach model with the grain size D90, which ranges between 0.38 mm to 2.13 mm across the study sites, for calculating the friction coefficient using the White-Colebrook formulation. The calibration of XBeach was carried out using a comprehensive sensitivity analysis based on the non-intrusive Polynomial Chaos Expansions method. Jamous et al.²⁵ calibrated the model for 12 sites (out of the 20 sites considered in the present study) and used the Brier Skill Score (BSS) to quantify the performance of the model⁵⁰.

The BSS measure considers the performance⁵⁰ of the model as bad if $BSS < 0$, poor if $0 < BSS < 0.3$, fair if $0.3 < BSS < 0.6$, good if $0.6 < BSS < 0.8$, and excellent if $0.8 < BSS < 1$. Most of the 12 sites' calibrated models showed excellent performance, with an average BSS of 0.82. We used the same calibration methodology as Jamous et al.²⁵ and calibrated the model for the remaining eight study sites (Profiles 216, 121, 122, 223, 128, 131, 133, 152). The average BSS of the calibrated sites is 0.72, with most profiles having a BSS above 0.6. The calibrated values of each parameter and the BSS value at each site are shown in Supplementary Table 1.

Given that the model is developed based on measurements from Hurricane Sandy, we use the pre-Sandy elevation profiles from Jamous et al.²⁵ as the initial beach-dune morphology in synthetic hurricane simulations. The assumption that the dune and the beach segment above the shoreline will remain unchanged in the future is justified by the fact that in developed

coastal regions such as our study area the beach-dune systems are regularly maintained to safeguard coastal residents and infrastructure. The shoreline position and the nearshore bathymetry are, however, subject to long-term evolution, which is not considered in the present study (see "Limitation" section for more details). Supplementary Fig. 2 shows the characteristics of pre-Sandy profiles. The beach-dune characteristics were calculated based on the location of the shoreline, and the front and back toes of the dune. The beach and dune volumes (Supplementary Fig. 2a) are calculated based on the beach and dune areas shown in Supplementary Fig. 3. The dune height (Supplementary Fig. 2b) is the elevation difference between the front toe and the crest of the dune. The beach slope (Supplementary Fig. 2c) is the slope of the best-fit line from the shoreline position (mean sea level) to the dune's front toe. The dune face slope (Supplementary Fig. 2c) is the slope of the best-fit line between the front toe and the crest of the dune. The beach and dune widths (Supplementary Fig. 2d) are the horizontal distances between the shoreline and the front toe, and the front and back toes, respectively.

Synthetic hurricanes and SLR scenario

The synthetic hurricanes are from tropical cyclone (TC) datasets used by Marsooli and Lin²⁶ and Marsooli et al.¹⁷, who studied climate change impacts on hurricane-induced storm surges and extreme waves. These synthetic storms were generated by the statistical/deterministic hurricane model of Emanuel et al.⁵ for the Atlantic basin. The hurricane model generates synthetic TCs for given large-scale atmospheric and oceanic conditions from observations or simulations by a GCM. While the model generates the storm genesis according to the statistics of historical storms, storm tracks from the genesis are predicted according to a corrected vertical average of the deep tropospheric environmental winds, which can be obtained from climate models or reanalysis. The model then estimates the wind field along the storm track using a computationally fast deterministic atmosphere-ocean model. Different datasets were generated for the climate conditions of the historical period of 1980–2000 and the future period of 2080–2100, under the RCP 8.5 scenario. Climate conditions were based on four different CMIP5 GCMs including Geophysical Fluid Dynamics Laboratory Climate Model, Coupled Physical Model CM3;⁵¹ Hadley Centre Global Environment Model, HadGEM5;^{52,53} Max-Planck-Institute for Meteorology Model, European Centre/Hamburg model ECHAM6;⁵⁴ and Meteorological Research Institute Model, Coupled General Circulation Model CGCM3⁵⁵.

Marsooli et al.¹⁷ used a validated regional-scale ADCIRC + SWAN model to simulate storm surges and waves generated by synthetic hurricanes from the above-mentioned storm datasets. They simulated major hurricanes, i.e., category 3, 4, and 5 hurricanes, that pass within a 500 km radius of the southern tip of Cape May County in the study area (see Fig. 1 for the location). The synthetic hurricane (categories 3–5) datasets and their corresponding annual frequencies are shown in Table 1, and their storm tracks are shown in Supplementary Fig. 4. The frequency of major hurricanes for the dataset i , f_i^{MH} , is calculated by multiplying the dataset's annual frequency of TCs by the ratio of the number of selected major hurricanes to the total number of TCs in that dataset. The ensemble frequency of major hurricanes is calculated based on weighting factors. The factor w for the dataset i is calculated as

$$w_i = \frac{N_i}{N} \quad (1)$$

where N_i is the number of selected major hurricanes from the dataset and N is the total number of selected major hurricanes from all four datasets. The ensemble frequency of major hurricanes is then calculated as $\sum w_i f_i^{MH}$.

Table 1. Synthetic major (category 3–5) hurricane datasets.

Dataset (Global Climate Models)	Historical Period 1980–2000		Future Period 2080–2100	
	Sample size	Frequency	Sample size	Frequency
HadGEM	267	0.05	397	0.134
CM3	13	0.002	63	0.04
ECHAM6	56	0.011	107	0.033
MRI-CGCM3	63	0.011	83	0.016
Ensemble	399	0.037	650	0.093

Frequency represents the annual frequency of storms that pass within a 500 km radius from the southern tip of Cape May County, New Jersey.

Marsooli et al.¹⁷ quantified the accuracy of synthetic hurricanes to represent the observed hurricane climatology by comparing the mean and 95th-percentile peak significant wave heights calculated from the climate model-based historical synthetic hurricanes and those calculated from the synthetic hurricanes generated for the historical observed climate (based on the National Centers for Environmental Prediction reanalysis, NCEP). They found a correlation coefficient of 0.98 and a normalized bias of 5% between the climate model- and NCEP-based historical synthetic major hurricanes. Their results showed a normalized root-mean-square-error of about 7 and 10% in the mean and 95th-percentile peak significant wave heights calculated from the climate model-based hurricanes.

To distinguish the effect of SLR on storm surges and waves from the effect of HCC, Marsooli et al.¹⁷ stimulated the future hurricanes under the historical Mean Sea Level (MSL) scenario as well as an SLR scenario of 1.19 m above the historical MSL. Under the RCP8.5 scenario, the selected SLR has a 50% chance of being equaled or exceeded in New Jersey by the end of the century¹². We use this SLR scenario for all study sites, given that projections show negligible differences in future SLR at different locations along the study region.

In the present study, we use storm surge and wave data from the ADCIRC + SWAN simulations by Marsooli et al.¹⁷ as boundary conditions of the XBeach model to simulate morphological changes to beach-dune systems. To force the XBeach model using the total water level rather than only the storm surge height, we added astronomical tide time series to the time series of synthetic hurricanes' storm surge heights. We set the timing of the largest tide at the Atlantic City tide gauge in the study area during historical Atlantic hurricane seasons (which is 1.09 m on 3 July 2000) to coincide with the peak storm surge and wave height during any synthetic storm.

At each site, a total of 1699 hurricanes are simulated, i.e., 399 simulations for the historical period, 650 simulations for the future period under the HCC scenario (i.e., no SLR), and 650 simulations for the future period under the HCC + SLR scenario. The effect of SLR in XBeach is accounted for by adding 1.19 m to the MSL used in the computational grids. The storm surge boundary conditions from Marsooli et al.¹⁷ are also relative to the future MSL. Marsooli et al.¹⁷ incorporated the sea level rise in ADCIRC + SWAN simulations by raising the vertical datum so that the bathymetry in the computational model was 1.19 m deeper. The storm surge outputs from the future storm simulations were relative to this new vertical datum.

Erosion hazard metrics

We consider the erosion hazard as the lost volume of sand from the beach-dune system. The following equation quantifies the percentage of Total Eroded Volume (TEV) above the shoreline

Table 2. Classification of storm-induced damage to beach-dune systems.

Damage Class	Definition
Major	Volume Change >40%
Moderate	Volume Change 5–40%
Minor	Volume Change <5%

(MSL = 0)

$$TEV = 100 \times \frac{V_E}{V} \quad (2)$$

where V is the total volume of sand in the beach-dune system above the historical mean sea level (see Supplementary Fig. 3 for areas of dune and beach), and V_E is the total volume of eroded sand, which is calculated based on the difference between the final (post-storm) and initial (pre-storm) bed elevations. The TEV metric is calculated for the beach-dune system as a whole as well as the beach and dune units separately.

Using the annual frequencies of the ensembled Hurricane dataset (Table 1) and TEV calculated from XBeach simulations, we estimate the return periods of TEV under historical and future climate conditions. The return period (RP) of TEV exceeding a given value h is calculated as

$$RP_{TEV}(h) = \frac{1}{f(1 - P\{TEV \leq h\})} \quad (3)$$

where f is the annual frequency and P is the cumulative probability distribution (CDF) of TEV, which is obtained by fitting an empirical CDF to the lower values of the calculated TEV and the Generalized Pareto Distribution (GPD) to the higher values (tail) of the TEV⁵⁶. An extreme value threshold is selected to distinguish lower values from extreme values of TEV and to fit the GPD return period curve. The threshold h is selected by trial and error so that the fitted return period curve accurately (with the lowest error) represents the extreme values of TEV. Here, we consider the 100-year TEV to be a proxy for extreme erosion. Then we calculate the percent change in the 100-year TEV (ΔTEV_{100-yr}) from historical to future periods to assess the impact of HCC and SLR on hurricane-induced erosion hazards.

The TEV metric is a useful lumped metric to quantify erosion hazards, but it does not provide an insight into the level of damage to the beach-dune system. Thus, we use a second metric to categorize the level of damage to beaches and dunes using the damage classification developed by Lemke and Miller³⁰, shown in Table 2. Although these categories were developed for dune damage, here we use them to separately quantify the level of damage for both dunes and beaches. We use the results of our simulations and the adopted damage classification to quantify the occurrence probability of each level of damage from historical to future periods. The probability is quantified as the ratio of the number of storms resulting in a certain damage class to the total number of storms in the historical or future periods.

LIMITATIONS

The present study assumed that the initial beach-dune elevation profiles in future periods would be the same as the historical initial profiles. In developed coastal regions like our study area, this assumption may be argued to be valid for the beach-dune portion that is above the shoreline, given that the beach-dune systems are well maintained to protect coastal communities and infrastructure. However, the shoreline position and nearshore seabed morphology are still subject to change due to short- and long-term coastal processes. Therefore, in addition to changes in extreme waves that were the focus of the present study, long-term changes in

shorelines and nearshore morphology would influence coastal erosion hazards. This may be achieved using process-based or data-driven models. With less reliability, simple empirical formulas, e.g., the Bruun Rule (for estimating sandy shoreline retreat due to changes in sea level), may be used as a first-order estimate of potential changes in shorelines. Studies that focus on intact or less developed regions should further account for the fact that beaches and dunes are also subject to morphologic evolution in response to sea level rise^{14,57,58}. Therefore, for such study regions, a coupled episodic-chronic morphological modeling approach will be needed to quantify the effects of HCC and SLR on coastal erosion hazards.

Astronomical tides can change the water depth in the nearshore zone over a short period of time. Changes in the water depth can affect the wave dynamics and consequently coastal processes, including erosion during extreme events. The present study assumed that the arrival time of peak storm surge and wave coincides with the highest tide in the study area, given that the study focused on the extreme end of a spectrum of coastal erosion hazards. Nevertheless, the arrival time of storms, relative to the tidal cycle, is rather random. For studies that aim to design coastal erosion mitigation strategies, the randomness of the tide timing compared to the peak storm surge and wave arrival time should be considered. This can be achieved by performing hydrodynamic-morphodynamic simulations of storms under various tide timing scenarios. However, this will result in a very large number of simulations and an increase in the computational cost by several factors.

We quantified erosion hazards of hurricanes that pass within 500 km from the southern tip of the study region. While the selected 500 km is subjective, it is aligned with the previous hurricane impact studies. In their investigation of changes to the characteristics of TC tracks that impact three major cities, Garner et al.⁵⁹ performed their analyses on TCs that traveled within 250 km of the study sites. Similarly, Garner et al.⁶⁰ studied coastal flood hazards in New York City under climate change by modeling storm surges from synthetic TCs that pass within 250 km of the city. Marsooli and Lin²⁶ investigated hurricane storm surge hazards in Jamaica Bay, New York, by hydrodynamic modeling of synthetic TCs that passed within a 200 km radius from the bay. Our selected hurricane impact radius of 500 km from the southern tip of the study region is larger than that from previous studies, assuring that all our study sites are within the commonly used storm impact domains. Our most northern study site (Profile 156) is about 150 km away from the most southern site (Profile 212). While we expect no significant changes in our results if the selected 500 km circular domain is shifted northward (due to the relatively limited extent of the study region), future research can perform a sensitivity analysis to quantify the optimum distance from the coast that can include all “impactful” offshore storms.

DATA AVAILABILITY

The results are available upon request from the authors.

CODE AVAILABILITY

XBeach and ADCIRC/SWAN models are open-source software that can be accessed at <https://oss.deltares.nl/web/xbeach/> and <https://adcirc.org/>, respectively.

Received: 4 February 2023; Accepted: 29 June 2023;
Published online: 11 July 2023

REFERENCES

- Lawrence, M. B., Mayfield, B. M., Avila, L. A., Pasch, R. J. & Rappaport, E. N. Atlantic hurricane season of 1995. *Mon. Weather Rev.* **126**, 1124–1151 (1998).
- Smith, A. B. & Katz, R. W. US billion-dollar weather and climate disasters: data sources, trends, accuracy and biases. *Nat. Hazards* **67**, 387–410 (2013).
- Vousdoukas, M. I. et al. Sandy coastlines under threat of erosion. *Nat. Clim. Change* **10**, 260–263 (2020).
- Spiske, M., Pilarczyk, J. E., Mitchell, S., Halley, R. B. & Otaï, T. Coastal erosion and sediment reworking caused by hurricane Irma – implications for storm impact on low-lying tropical islands. *Earth Surf. Process. Landf.* **47**, 891–907 (2022).
- Emanuel, K., Sundararajan, R. & Williams, J. Hurricanes and global warming: results from downscaling IPCC AR4 simulations. *Bull. Am. Meteorol. Soc.* **89**, 347–368 (2008).
- Hill, K. A. & Lackmann, G. M. The impact of future climate change on TC intensity and structure: a downscaling approach. *J. Clim.* **24**, 4644–4661 (2011).
- Knutson, T. et al. Dynamical downscaling projections of twenty-first-century atlantic hurricane activity: CMIP3 and CMIP5 model-based scenarios. *J. Clim.* **26**, 6591–6617 (2013).
- Knutson, T. R. et al. Global projections of intense tropical cyclone activity for the late twenty-first century from dynamical downscaling of CMIP5/RCP4.5 scenarios. *J. Clim.* **28**, 7203–7224 (2015).
- Walsh, K. J. E. et al. Tropical cyclones and climate change. *Wiley Interdiscip. Rev. Clim. Change* **7**, 65–89 (2016).
- Sugi, M., Murakami, H. & Yoshida, K. Projection of future changes in the frequency of intense tropical cyclones. *Clim. Dyn.* **49**, 619–632 (2017).
- Arias, P. et al. *Climate Change 2021: The Physical Science Basis. Contribution of Working Group I to the Sixth Assessment Report of the Intergovernmental Panel on Climate Change; Technical Summary* 33–144 (IPCC, 2021).
- Kopp, R. E. et al. *New Jersey's Rising Seas and Changing Coastal Storms: Report of the 2019 Science and Technical Advisory Panel*. 46 (2019). <https://doi.org/10.7282/T3-EEQR-MQ48>.
- Fox-Kemper, B. et al. *Ocean, Cryosphere and Sea Level Change. In Climate Change 2021: The Physical Science Basis. Contribution of Working Group I to the Sixth Assessment Report of the Intergovernmental Panel on Climate Change* (eds. Masson-Delmotte, V., P. Zhai, A. Pirani, S. L. Connors, C. Péan, S. Berger, N. Caud, Y. Chen, L. Goldfarb, M. I. Gomis, M. Huang, K. Leitzell, E. Lonnoy, J. B. R. Matthews, T. K. Maycock, T. Waterfield, O. Yelekçi, R. Yu, and B. Zhou) (Cambridge University Press, 2021).
- Zhang, K., Douglas, B. C. & Leatherman, S. P. Global warming and coastal erosion. *Clim. Change* **64**, 41–58 (2004).
- Lin, N., Kopp, R. E., Horton, B. P. & Donnelly, J. P. Hurricane Sandy's flood frequency increasing from year 1800 to 2100. *Proc. Natl Acad. Sci. USA* **113**, 12071–12075 (2016).
- Marsooli, R., Lin, N., Emanuel, K. & Feng, K. Climate change exacerbates hurricane flood hazards along US Atlantic and Gulf Coasts in spatially varying patterns. *Nat. Commun.* **10**, 3785 (2019).
- Marsooli, R., Jamous, M. & Miller, J. K. Climate change impacts on wind waves generated by major tropical cyclones off the coast of New Jersey, USA. *Front. Built Environ.* **7**, 161 (2021).
- Taherkhani, M. et al. Sea-level rise exponentially increases coastal flood frequency. *Sci. Rep.* **10**, 6466 (2020).
- Ranasinghe, R., Callaghan, D. & Stive, M. J. F. Estimating coastal recession due to sea level rise: beyond the Bruun rule. *Clim. Change* **110**, 561–574 (2012).
- Cooper, J. A. G. et al. Sandy beaches can survive sea-level rise. *Nat. Clim. Change* **10**, 993–995 (2020).
- Kriebel, D. L. & Dean, R. G. Numerical simulation of time-dependent beach and dune erosion. *Coast. Eng.* **9**, 221–245 (1985).
- De Winter, R. C. & Ruessink, B. G. Sensitivity analysis of climate change impacts on dune erosion: case study for the Dutch Holland coast. *Clim. Change* **141**, 685–701 (2017).
- Tang, Q. et al. The Fully Coupled Regionally Refined Model of E3SM Version 2: Overview of the Atmosphere, Land, and River. Preprint at <https://gmd.copernicus.org/preprints/gmd-2022-262/> (2022).
- Gori, A., Lin, N., Xi, D. & Emanuel, K. Tropical cyclone climatology change greatly exacerbates US extreme rainfall–surge hazard. *Nat. Clim. Change* **12**, 171–178 (2022).
- Jamous, M., Marsooli, R. & Ayyad, M. Global sensitivity and uncertainty analysis of a coastal morphodynamic model using Polynomial Chaos Expansions. *Environ. Model. Softw.* **160**, 105611 (2023).
- Marsooli, R. & Lin, N. Impacts of climate change on hurricane flood hazards in Jamaica Bay, New York. *Clim. Change* **163**, 2153–2171 (2020).
- Lemke, L. & Miller, J. K. Evaluation of storms through the lens of erosion potential along the New Jersey, USA coast. *Coast. Eng.* **158**, 103699 (2020).
- Harley, M. D. et al. Extreme coastal erosion enhanced by anomalous extratropical storm wave direction. *Sci. Rep.* **7**, 6033 (2017).
- Colle, B. A., Booth, J. F. & Chang, E. K. M. A review of historical and future changes of extratropical cyclones and associated impacts along the US East Coast. *Curr. Clim. Change Rep.* **1**, 125–143 (2015).

30. Lemke, L. & Miller, J. K. Role of storm erosion potential and beach morphology in controlling dune erosion. *J. Mar. Sci. Eng.* **9**, 1428 (2021).
31. Zappa, G., Shaffrey, L., Hodges, K., Sansom, P. & Stephenson, D. A multimodel assessment of future projections of north atlantic and european extratropical cyclones in the CMIP5 climate models. *J. Clim.* **26**, 5846–5862 (2013).
32. Seiler, C. & Zwiers, F. W. How will climate change affect explosive cyclones in the extratropics of the Northern Hemisphere? *Clim. Dyn.* **46**, 3633–3644 (2016).
33. Champion, A. J., Hodges, K. I., Bengtsson, L. O., Keenlyside, N. S. & Esch, M. Impact of increasing resolution and a warmer climate on extreme weather from Northern Hemisphere extratropical cyclones. *Tellus A: Dyn. Meteorol. Oceanogr.* **63**, 893–906 (2011).
34. Priestley, M. D. K. & Catto, J. L. Future changes in the extratropical storm tracks and cyclone intensity, wind speed, and structure. *Weather Clim. Dyn.* **3**, 337–360 (2022).
35. Jing, R., Lin, N., Emanuel, K., Vecchi, G. & Knutson, T. R. A comparison of tropical cyclone projections in a high-resolution global climate model and from downscaling by statistical and statistical-deterministic methods. *J. Clim.* **34**, 9349–9364 (2021).
36. Santos, V. M., Wahl, T., Long, J. W., Passeri, D. L. & Plant, N. G. *Coastal Sediments 2019*. p. 1327–1339 (WORLD SCIENTIFIC, 2019).
37. Athanasiou, P. et al. Estimating dune erosion at the regional scale using a meta-model based on neural networks. *Nat. Hazards Earth Syst. Sci.* **22**, 3897–3915 (2022).
38. Roelvink, D. et al. Modelling storm impacts on beaches, dunes and barrier islands. *Coast. Eng.* **56**, 1133–1152 (2009).
39. McCall, R. T. et al. Two-dimensional time dependent hurricane overwash and erosion modeling at Santa Rosa Island. *Coast. Eng.* **57**, 668–683 (2010).
40. Splinter, K. D. & Palmsten, M. L. Modeling dune response to an East Coast Low. *Mar. Geol.* **329–331**, 46–57 (2012).
41. Kalligeris, N., Smit, P. B., Ludka, B. C., Guza, R. T. & Gallien, T. W. Calibration and assessment of process-based numerical models for beach profile evolution in southern California. *Coast. Eng.* **158**, 103650 (2020).
42. Luettich, J., Richard, Westerink, J. & Scheffner, N. ADCIRC: An Advanced Three-Dimensional Circulation Model for Shelves, Coasts, and Estuaries. Report 1. Theory and Methodology of ADCIRC-2DDI and ADCIRC-3DL. *Dredging Research Program Tech. Rep. DRP-92-6*. p. 143 (1992).
43. Westerink, J., Luettich, J., Richard, Blain, C. & Scheffner, N. ADCIRC: An Advanced Three-Dimensional Circulation Model for Shelves, Coasts, and Estuaries. Report 2. User's Manual for ADCIRC-2DDI. 168 (1994).
44. Booij, N., Ris, R. C. & Holthuijsen, L. H. A third-generation wave model for coastal regions: 1. Model description and validation. *J. Geophys. Res. Oceans* **104**, 7649–7666 (1999).
45. Ris, R., Booij, N. & Holthuijsen, L. A third-generation wave model for coastal regions: 2. Verification. *J. Geophys. Res.* **104**, 7667–7681 (1999).
46. Blake, E. S. *Tropical Cyclone Report: Hurricane Sandy*. (DIANE Publishing Company, 2013).
47. Herrington, T. From the Editor's Desk: Learning the lessons of Sandy. *Shore Beach* **84**, 2–4 (2016).
48. Sopkin, K. L. et al. *Hurricane Sandy: Observations And Analysis Of Coastal Change* (US Department of the Interior, US Geological Survey, 2014).
49. Flynn, M. J. *Sediment Characterization Of The New Jersey Shoreline: Comparison Of Median Grain Size Distribution From 1950 to 2011* (The Richard Stocton College Coastal Research Center, 1999).
50. van Rijn, L. C. et al. The predictability of cross-shore bed evolution of sandy beaches at the time scale of storms and seasons using process-based Profile models. *Coast. Eng.* **47**, 295–327 (2003).
51. Donner, L. J. et al. The dynamical core, physical parameterizations, and basic simulation characteristics of the atmospheric component AM3 of the GFDL global coupled model CM3. *J. Clim.* **24**, 3484–3519 (2011).
52. Collins, W. J. et al. Development and evaluation of an Earth-System model – HadGEM2. *Geosci. Model Dev.* **4**, 1051–1075 (2011).
53. The HadGEM2 Development Team, Martin, G. M. et al. The HadGEM2 family of Met Office Unified Model climate configurations. *Geosci. Model Dev.* **4**, 723–757 (2011).
54. Stevens, B. et al. Atmospheric component of the MPI-M Earth System Model: ECHAM6. *J. Adv. Model. Earth Syst.* **5**, 146–172 (2013).
55. Yukimoto, S. et al. A new global climate model of the meteorological research institute: MRI-CGCM3 —model description and basic performance. *J. Meteorol. Soc. Jpn Ser. II* **90A**, 23–64 (2012).
56. Coles, S. *An Introduction to Statistical Modeling of Extreme Values*. (Springer, 2001).
57. Mentaschi, L., Voudoukas, M. I., Pekel, J.-F., Voukouvalas, E. & Feyen, L. Global long-term observations of coastal erosion and accretion. *Sci. Rep.* **8**, 12876 (2018).
58. Schuerch, M. et al. Future response of global coastal wetlands to sea-level rise. *Nature* **561**, 231–234 (2018).
59. Garner, A. J., Kopp, R. E. & Horton, B. P. Evolving Tropical Cyclone Tracks in the North Atlantic in a Warming Climate. *Earth's Future* **9**, 1–16 (2021).
60. Garner, A. J. et al. Impact of climate change on New York City's coastal flood hazard: Increasing flood heights from the preindustrial to 2300 CE. *Proc. Natl Acad. Sci. USA* **114**, 11861–11866 (2017).

ACKNOWLEDGEMENTS

This publication is the result of work sponsored by the New Jersey Sea Grant with funds from the National Oceanic and Atmospheric Administration (NOAA) Office of Sea Grant, U.S. Department of Commerce, under NOAA grant #NA18OAR4170087 and the New Jersey Sea Grant Consortium. The statements, findings, conclusions, and recommendations are those of the author(s) and do not necessarily reflect the views of New Jersey Sea Grant or the U. S. Department of Commerce. NJSJG-22-1009. We would like to thank the Coastal Research Center at Stockton University for providing the Post- and Pre-Hurricane Sandy elevation measurements used in the calibration of the XBeach model.

AUTHOR CONTRIBUTIONS

R.M. designed the study and M.J. performed the numerical simulations and analyzed the results. R.M. supervised numerical simulations, and R.M. and J.K.M. supervised data analysis. All authors discussed the results. M.J. wrote the first draft of the paper and R.M. edited the paper. All authors were involved in the scientific interpretation and reviewed the paper.

COMPETING INTERESTS

The authors declare no competing interests.

ADDITIONAL INFORMATION

Supplementary information The online version contains supplementary material available at <https://doi.org/10.1038/s41612-023-00416-0>.

Correspondence and requests for materials should be addressed to Reza Marsooli.

Reprints and permission information is available at <http://www.nature.com/reprints>

Publisher's note Springer Nature remains neutral with regard to jurisdictional claims in published maps and institutional affiliations.



Open Access This article is licensed under a Creative Commons Attribution 4.0 International License, which permits use, sharing, adaptation, distribution and reproduction in any medium or format, as long as you give appropriate credit to the original author(s) and the source, provide a link to the Creative Commons license, and indicate if changes were made. The images or other third party material in this article are included in the article's Creative Commons license, unless indicated otherwise in a credit line to the material. If material is not included in the article's Creative Commons license and your intended use is not permitted by statutory regulation or exceeds the permitted use, you will need to obtain permission directly from the copyright holder. To view a copy of this license, visit <http://creativecommons.org/licenses/by/4.0/>.

© The Author(s) 2023